ESA Climate Change Initiative Phase II - Soil Moisture

Algorithm Theoretical Baseline Document (ATBD) D2.1 Version 04.4

Merging Active and Passive Soil Moisture Retrievals

12 November 2018

Prepared by

Earth Observation Data Centre for Water Resources Monitoring (EODC) GmbH

in cooperation with

TU Wien, GeoVille, ETH Zürich, TRANSMISSIVITY, AWST, FMI, UCC and NILU

This document forms part 4 (of 4) of deliverable D2.1 Algorithm Theoretical Baseline Document (ATBD) and was compiled for the ESA Climate Change Initiative Phase 2 Soil Moisture Project (ESA Contract No.4000112226/14/I-NB). For more information on the CCI programme of the European Space Agency (ESA) see http://www.esa-cci.org/.

Number of pages: 41

Authors:	D. Chung, W. Dorigo, S. Hahn. T. Melzer. C. Paulik. C. Reimer, M. Vreugdenhil, W. Wagner, R. Kidd, A. Gruber, T. Scanlon		
Circulation:	Public release		
Release	Date	Details	Editor
0.1	30/11/2015	Revision to match ESA CCI SM v02.2 release	D. Chung
0.2	04/12/2015	Editing + typesetting	W Dorigo
3.2	01/12/2016	Revision to match ESA CCI SM v03.2 release	D. Chung, W. Dorigo
3.2	24/02/2017	Minor update	D. Chung, A. Gruber
3.3	10/11/2017	Update to product version 03.3	T. Scanlon
4.2	15/01/2018	Update to product version 04.2	A. Gruber, T. Scanlon
4.3	17/04/2018	Update to product version 04.3 (not publically released)	T. Scanlon
4.4	12/11/2018	Update to product version 04.4 (data extension). Added details of changes in input datasets and information on flagging for high vegetation (temporal resampling section).	P. Buttinger T. Scanlon

For any clarifications please contact Wouter Dorigo (wouter.dorigo@geo.tuwien.ac.at).

Project Partners

Prime Contractor **Scientific Lead**	**EODC,** Earth Observation Data Centre for Water Resources Monitoring (Austria)
Project Management	**GeoVille**, GeoVille Information Systems GmbH (Austria)
System Engineering Partners	**AWST**, Angewandte Wissenschaft Software und Technologie GmbH (Austria)
Earth Observation Partners	**TU Wien**, Vienna University of Technology (Austria) **TMS**, Transmissivity, (The Netherlands) **FMI**, Finnish Meteorological Institute, (Finland) **UCC**, University College Cork, (Ireland)
Climate Research Partners	**ETH**, Institute for Atmospheric and Climate Science, (Switzerland) **NILU**,Norsk institutt for luftforskning (Norway)

Table of Content

List of Figures

List of Tables

Definitions, acronyms and abbreviations

AMI	Active Microwave Instrument
AMSR-E	Advanced Microwave Scanning Radiometer-Earth Observing System
AMSU	Advanced Microwave Sounding Unit
ASAR	Advanced Synthetic Aperture Radar
ASCAT	Advanced Scatterometer (Metop)
CCI	Climate Change Initiative
CEOP	Coordinated Energy and Water Cycle Observations Project
CMORPH	Morphing Method of the Climate Prediction Centre
CPC	Climate Prediction Centre
DARD	Data Access Requirement Document
DMSP	Defence Meteorological Satellite Program
DTED	Digital Terrain Elevation Model
EASE	Equal-Area Scalable Earth
ECV	Essential Climate Variable
ENVISAT	Environmental Satellite
EO	Earth Observation
ERA-40	ECMWF ReAnalysis 40 data set
ERS	European Remote Sensing Satellite (ESA)
EUMETSAT	European Organisation for the Exploitation of Meteorological Satellites
FTP	File Transfer Protocol
GIMMS	Global Inventory Modeling and Mapping Studies
GLDAS	Global Land Data Assimilation System
GLWD	Global Lakes and Wetlands Database (GSPC/University of Kassel)
GPCC	Global Precipitation Climatology Centre

GPCP	Global Precipitation Climatology Project
GRACE	Gravity Recovery And Climate Experiment
GSWP	Global Soil Wetness Project
ISMN	International Soil Moisture Network
ITRDB	International Tree-Ring Data Bank
JAXA	(Japan Aerospace Exploration Agency)
JPL	Jet Propulsion Laboratory (NASA)
METOP	Meteorological Operational Satellite (EUMETSAT)
NASA	National Aeronautics and Space Administration
NIMA	National Imagery and Mapping Agency
NOAA	National Oceanic and Atmospheric Administration
NSIDC	National Snow and Ice Data Center (radlab)
NWS	National Weather Service (NOAA)
SAR	Synthetic Aperture Radar
SCAT	Scatterometer
SMAP	Soil Moisture Active and Passive mission
SMMR	Scanning Multichannel Microwave Radiometer
SMOS	Soil Moisture and Ocean Salinity (ESA)
SNR	Signal to Noise Ratio
SOW	Statement of Work
SSM	Surface Soil Moisture
SSM/I	Special Sensor Microwave Imager
TDR	Time Domain Reflectometry
TMI	TRMM Microwave Imager
TRMM	Tropical Rainfall Measuring Mission
TWS	Terrestrial Water Storage
USGS	United States Geological Survey
VIC	Variable Infiltration Capacity
VOD	Vegetation Optical Depth
WACMOS	Water Cycle Multimission Observation Strategy
WindSat	WindSat Radiometer

List of symbols

θ	Incidence angle (degree), generic
$\theta_{i,b}$	Observed incidence angle of beam $b \in \{f, m, a\}$ (fore-, mid-, aft-beam) of i-th record in the time series of the current GPI
$\varphi, \varphi_{i,b}$	Azimuth angle (degree), generic and observed
$\sigma^0, \sigma^0_{i,b}$	Radar cross-section, backscattering coefficient $\left(\frac{m^2}{m^2} \text{ or } dB\right)$, generic and observed
t, t_i	Time, generic and observed
$d = doy(t), d_i$	Day of year, $d \in \mathbb{N}, 1 \leq d \leq 366$, as function of t (t_i)
$\sigma^0(\theta, d)$	Backscatter, modelled as function of incidence angle, with the model depending on the day of year d (i.e., d indexes one instance of the model class)
$\sigma^0_{i,b}(\theta_i)$	Observed backscatter, represented in terms of the model
$\sigma'(\theta, d)$	First derivative of $\sigma^0(\theta, d)$
$\sigma'(\theta_{ref}, d)$	First derivative ('slope') at reference angle, parameter array
$\sigma''(\theta, d)$	Second derivative of $\sigma^0(\theta, d)$
$\sigma''(\theta_{ref}, d)$	Second derivative ('curvature') at reference angle, parameter array
$\overline{\sigma^0_i}(\theta_{ref})$	Normalised backscatter at reference angle, averaged over the beams, of the i-th record in the time series
θ_{dry}	Dry crossover angle
$\sigma^{dry}(\theta_{ref}, d)$	Dry reference at reference angle, parameter array
θ_{wet}	Wet crossover angle
$\sigma^{wet}(\theta_{ref}, d)$	Wet reference at reference angle, parameter array

1 Executive Summary

The Algorithm Theoretical Baseline Document (ATBD) provides a detailed description of the algorithms that are used within the ESA CCI Soil Moisture production system. The ESA CCI SM production system was initially developed within CCI Phase 1 and is continuously being updated within phase 2 to reflect the current state of the science driving the system. The ATBD is, by its nature, rather in-depth, and in order to facilitate frequent updates, and to provide a more manageable document to the reader the ATBD is provided as four distinct documents. These documents consist of an ATBD for the active retrieval, an ATBD for the passive retrieval and an ATBD for the merging process. An overriding document (part 1) provides an executive summary which sets the ATBD documents within framework for the CCI project and the ESA CCI SM production system.

Section 2 summarises the algorithmic and main processor changes that were implemented to update ESA CCI SM v03.3 to the current version v04.4. With regards to v04.2, v004.4 has no algorithmic changes; in v04.4, the temporal coverage of the dataset is extended to 30-06-2018 (previously, at v04.2, the dataset covered to 31-12-2017).

The core of this document is provided in Section 5, which provides a general overview of the merging procedure and the commonalities between different modules. Section 5 describes the single algorithms in detail. The system involves three steps: (1) merging the original active microwave soil moisture products into a single product (period 1991 – 2018) called ACTIVE, (2) merging the original passive microwave soil moisture products into a passive ECV (1978 – now) labelled as PASSIVE, and (3) combining the two merged products into an active + passive ECV (1978 – 2018) named COMBINED. Before merging can take place all input datasets are resampled to a common grid and time stamp. As the input datasets have different dynamic ranges (e.g. due to differences in unit or sensor specifications) they need to be rescaled into a common climatology. This is done by CDF-matching. As a result, PASSIVE is expressed in the dynamic range of the AMSR-E product and ACTIVE in that of ASCAT. As no observational dataset has a global coverage, GLDAS-Noah land surface model soil moisture estimates serve as a reference for scaling ACTIVE and PASSIVE into a common climatology. Finally, merging the rescaled ACTIVE and PASSIVE products into COMBINED follows a scheme which takes into account the differences in relative performance over space and time.

Section 7 recapitulates the shortcomings of the existing ESA CCI SM production chain and by outlining the research that is needed to fill these gaps. The scientific advances that are currently carried out to fill these gaps are described in Section 8.

2 Change log

2.1 Current version 04.4

This document forms deliverable 2.1 of CCI Phase 2 and provides an update for the ESA CCI SM 04.4 product released on 12th November 2018. The main differences between version 04.4 and the previously used version 3 algorithm (public releases were versions v03.2 and v03.3) are summarised below.

- GLDAS-Noah soil temperature and Snow Water Equivalent estimates are now used to mask out unreliable retrievals before CDF-Matching (COMBINED only) and TC error estimation (all products).
- All data sets are now rescaled against GLDAS v1 due to inconsistencies between v1 and v2.0 (COMBINED only)
- "Frozen" flags of active products are now used to mask out unreliable retrievals in the passive products and vice versa (COMBINED only)
- Update of AMSR2 data
- Correction of incorrect metadata in netCDF images (LPRMv06 are used for AMSRE, SMOS, and AMSR2 since ESA CCI SM v03.2)
- The COMBINED product is now generated by merging all active and passive L2 products directly (after CDF-matching against GLDAS-Noah) instead of merging the pre-merged ACTIVE and PASSIVE products (as it was the case up until ESA CCI SM v03.3).
- Uncertainty estimates for all L2 products in regions where triple collocation analysis (TCA) does not provide reliable estimates are now available (and used for calculating relative weights) obtained through a regression between Vegetation Optical Depth (VOD) and Signal-to-Noise Ratio (SNR) estimates in all regions where TCA is deemed reliable

The main change between v04.2 and v04.4 is the temporal extension to end of June 2018 (note version 4.3 is not discussed here as it was not released to the public). Whilst there were no changes to the algorithm used, there were changes to the made to the input data and the processor; without these changes the temporal extension would not be possible due to the unavailability of the input data.

- GLDAS v1 was only available to the end of 2016, therefore, this has been replaced with GLDAS v2.1[1]. The data is used as the reference in both the scaling and triple collocation stages.
- Passive data from LPRM v6 is used for SMOS, AMSR2 and AMSR-E. Whilst this was also the case in the previous version (v04.2), the flagging of high has been modified.

[1] GLDAS v2.1: https://disc.gsfc.nasa.gov/datasets/GLDAS_NOAH025_3H_V2.1/summary?keywords=GLDAS

Previously this was based on a threshold of 0.5 for all LPRM v6 products and now it is based on an assessment for each band of each sensor. Further details are provided in Section 6.1.2.

- During the SNR gap-filling stage, a VOD map is used as part of the regression analysis. Previously, this VOD map has been based on LPRM v5 data from AMSR-E C-band data between 2002 and 2011 (mean VOD is calculated). This data has now been updated with the equivalent data from LPRM v6.
- The temporal extension to the ASCAT data is provided by a combination of the following two products while previously (at v04.2), the H111 product was utilised:
    - WARP 5.8.0/H113/ASCAT/MetOp-A/B DR2017 SSM time series 12.5 km sampling
    - WARP 5.8.0/H114/ASCAT/MetOp-A/B DR2018 EXT SSM time series 12.5 km sampling

2.2 Pre v04.4

The dataset and corresponding ATBD versions are summarised in the executive summary of the ATBD. Further information can be found in the changelog provided with the data and the relevant documentation.

3 Introduction

3.1 Purpose of the Document

The Algorithm Theoretical Baseline Document (ATBD) is intended to provide a detailed description of the scientific background and theoretical justification for the algorithms used to produce the ECV soil moisture data sets. Furthermore, it describes the scientific advances and algorithmic improvements which are made within the CCI project.

3.2 Targeted Audience

This document targets mainly:

- Remote sensing experts and scientists that are interested in the retrieval and error characterisation of the ECV_SM blended soil moisture products from active and passive microwave data sets.
- Climate scientists that are interested in the properties and accuracy of the ECV_SM products over time.

4 Reference Documents

The following references are of relevance to this document. Within the document, for the sake of clarity it has been sometimes necessary to provide sections of quoted texts taken from referenced documents, rather than just providing a reference to the document. In these cases, texts are "*presented in quotes as italic text*".

[RD-1]	ESA Climate Change Initiative Phase 1, Statement of Work for Soil Moisture and Ice Sheets, European Space Agency, EOEP-STRI-EOPS-SW-11-0001.
[RD-2]	Technical Proposal (Part 3) in response to ESA Climate Change Initiative Phase 1 ESRIN/AO/1-6782/11/I-NB, Vienna University of Technology.
[RD-3]	W. Dorigo, R. Kidd, R. De Jeu, S. Seneviratne, H. Mittelbach, J. Pulliainen, W.A. Lahoz, N. Dwyer, B. Barrett, Eva Haas, W. Wagner.ESA CCI Soil Moisture Data Access Requirements Document, v1.2
[RD-4]	Wagner, W., W. Dorigo, R. De Jeu, D. Fernandez, J. Benveniste, E. Haas, M. Ertl (2012) Fusion of active and passive microwave observations to create an Essential Climate Variable data record on soil moisture, Proceedings of the ISPRS Congress 2012, Melbourne, Australia, August 25-September 1, 2012.
[RD-5]	Liu, Y. Y., Parinussa, R. M., Dorigo, W. A., De Jeu, R. A. M., Wagner, W., van Dijk, A. I. J. M., McCabe, M. F., Evans, J. P. (2011). Developing an improved soil moisture dataset by blending passive and active microwave satellite-based retrievals. Hydrology and Earth System Sciences, 15, 425-436, doi:10.5194/hess-15-425-2011
[RD-6]	Liu, Y.Y., Dorigo, W.A., Parinussa, R.M., de Jeu, R.A.M., Wagner, W., McCabe, M.F., Evans, J.P., van Dijk, A.I.J.M. (2012). Trend-preserving blending of passive and active microwave soil moisture retrievals, Remote Sensing of Environment, 123, 280-297, doi: 10.1016/j.rse.2012.03.014.
[RD-7]	D. Chung, R.A.M de Jeu, W. Dorigo, S. Hahn. T. Melzer. R.M. Parinussa, C. Paulik. C. Reimer, M. Vreugdenhil, W. Wagner (2012). ESA CCI Soil Moisture. Algorithm Theoretical Baseline Document (ATBD), Version 0, 30th April 2012.
[RD-8]	D. Chung, R.A.M de Jeu, W. Dorigo, S. Hahn. T. Melzer. R.M. Parinussa, C. Paulik. C. Reimer, M. Vreugdenhil, W. Wagner (2013), Algorithm Theoretical Baseline Document (ATBD), Version 1.0, release 1.0, 14th February 2013.
[RD-9]	D. Chung, W. Dorigo, S. Hahn. T. Melzer. C. Paulik. C. Reimer, M. Vreugdenhil, W. Wagner, R. Kidd (2013). Soil Moisture Retrieval from Active Microwave Sensors:

	Algorithm Theoretical Baseline Document (ATBD) Version 2.0, Release 0.3, 15th October 2014.
[RD-10]	D. Chung, R.A.M. de Jeu, W. Dorigo, S. Hahn. T. Melzer. R.M. Parinussa, C. Paulik. C. Reimer, M. Vreugdenhil, W. Wagner, R. Kidd (2013). ESA CCI Soil Moisture – Soil Moisture Retrieval from Passive Microwave Sensors: Algorithm Theoretical Baseline Document (ATBD), Version 2.0, Release 0.4, 15th October 2014.
[RD-11]	D. Chung, W. Dorigo, S. Hahn. T. Melzer. C. Paulik. C. Reimer, M. Vreugdenhil, W. Wagner, R. Kidd (2013). ESA CCI Soil Moisture – ECV production, Fusion of Soil Moisture Products: Algorithm Theoretical Baseline Document (ATBD) Version 2.0 Release 0.5, 15th October 2014.
[RD-12]	R. Kidd, D. Chung, W. Dorigo, R. De Jeu (2013). ESA CCI Soil Moisture – Detailed Processing Model (DPM), Version 1.2, 26th November 2013.
[RD-13]	D. Chung R. Kidd, W. Dorigo (2013) ESA CCI Soil Moisture – System Prototype Description (SPD), Version 1.0, 4th July 2013.
[RD-14]	R. Kidd, D. Chung, W. Dorigo, R. De Jeu (2012). Input/ Output Data Definition Document (IODD), Version 1.0, 21st December 2012.

5 Methodological description on the merging process of soil moisture data sets

5.1 Principle of the merging process

The generation of the long-term (39+ years) soil moisture data set involves three steps (Figure 1):

(1) merging the original passive microwave soil moisture products into one product,
(2) merging the original active microwave soil moisture products into one product, and
(3) merging all original active and passive microwave soil moisture products into one dataset.

The input datasets considered for the generating and validating the merged soil moisture product are:

- Scatterometer-based soil moisture products
  - Sensors: ERS-1/2 and MetOp-A ASCAT, MetOp-B ASCAT
  - Retrieval method: change detection method TU Wien WARP v5.8.0
  - Time span: 1991 – 2018
- Radiometer-based soil moisture products
  - Sensors: SMMR, SSM/I, TRMM, AMSR-E, AMSR2, Windsat, and SMOS
  - Retrieval method: VUA-NASA LPRM v5 / v6 model inversion package
  - Time span: 1978 – 2018
- Modelled 0 – 10 cm soil moisture from the Noah land surface model of the Global Land Data Assimilation System (GLDAS; (Rodell et al. 2004)).
  - v2.1: Time span: 2000 – 2018 (0.25 degree resolution)
  - v2.0: Time span: 1948 – 2000 (0.25 degree resolution)
- In situ measurements:
  - Various networks: ESA/TU Wien International Soil Moisture Network (http://ismn.geo.tuwien.ac.at)
  - Time period: variable depending on station
  - Probes and depths: variable depending on station

The homogenised and merged products represent surface soil moisture with a global coverage and a spatial resolution of 0.25°. The time period spans the entire period covered by the individual sensors, i.e. 1978 – 2018, while measurements are provided at a 1-day sampling.

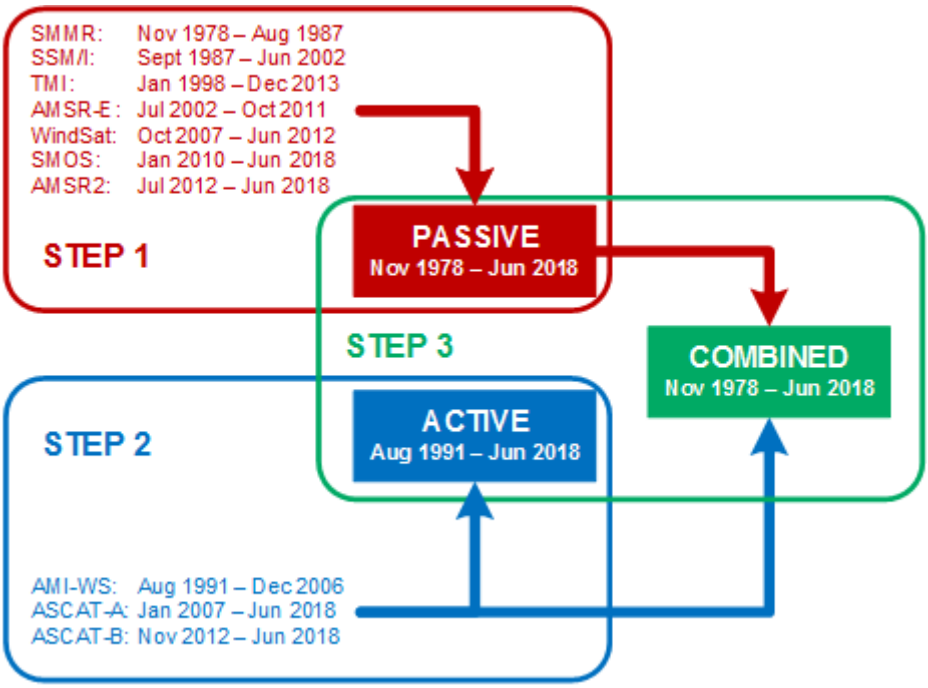

Figure 1: Overview of the three-step blending approach from original products to the final blended active & passive microwave soil moisture product for ESA CCI SM v04.4. (Adapted from (Liu et al. 2012)).

5.2 Overview of processing steps

The level 2 surface soil moisture products derived from the active and passive remotely sensed data undergo a number of processing steps in the merging procedure (see Figure 2 for an overview):

1. Spatial Resampling
2. Temporal Resampling (including flagging of observations)
3. Rescaling passive and active level 2 observations into radiometer and scatterometer climatologies (for the ACTIVE and PASSIVE product), , and separately rescaling all level 2 observations into a common climatology (for the COMBINED product)
4. Triple collocation analysis (TCA) based error characterisation of all rescaled level 2 products
5. Polynomial regression between VOD and error estimates
6. Derivation of error estimates from the VOD regression in regions where they were not available after (4), i.e., where TCA is deemed unreliable
7. Merging rescaled passive and active time series into the PASSIVE,ACTIVE, and COMBINED product, respectively

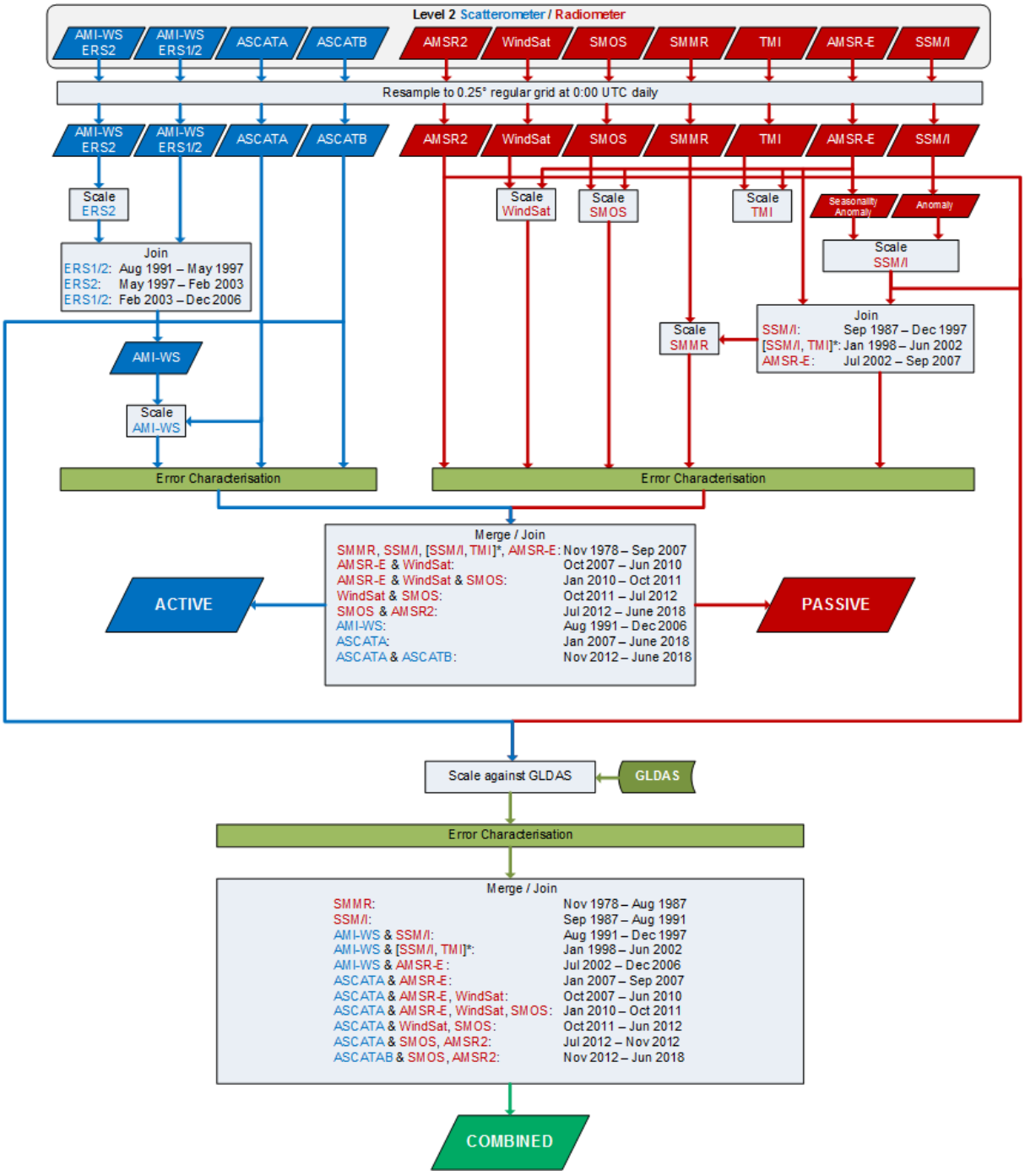

Figure 2: *Overview of the processing steps in the ESA CCI SM product generation (v04.4): The merging of two or more data sets is done by weighted averaging and involves overlapping time periods, whereas the process of joining data sets only concatenates two or more data sets between the predefined time periods. The join process is performed on datasets of each lines and on datasets separated by comma within the rectangular process symbol. *The [SSM/I, TMI] period is specified not only by the temporal, but also by the spatial latitudinal coverage (see Figure 8).*

6 Description of Algorithms

In this section the algorithms of the scaling and merging approach are described. Notice that several algorithms, e.g. rescaling, are used in various steps of the process, but will be described only once

6.1 Resampling

The sensors used for the different merged products have different technical specifications (Table 3). Obvious are the differences in spatial resolution and crossing times. Both elements need to be brought into a common reference before the actual merging can take place.

6.1.1 Spatial Resampling

The merged products are provided on a regular grid with a spatial resolution of 0.25° in both latitude and longitude extension. This is a trade-off between the higher resolution scatterometer data and the generally coarser passive microwave observations without leading to any undersampling. The resolution of the products is often adopted by land surface models. Nearest neighbour resampling is performed on the radiometer input data sets to bring them into the common regular grid. Following this resampling technique each grid point in the reference (regular grid) data set is assigned to the value of the closest grid point in the input dataset. In general, the nearest neighbour resampling algorithm can be applied to data set with regular degree grid. For the active microwave data sets, where equidistant grid points are defined by the geo-reference location of the observation, the hamming window function is used to resample the input data to a 0.25° regular grid. The search radius is a function of latitude of the observation location, as the distance between two regular grid points reduces as the location tends towards the poles. In contrast, the active microwave data set uses the DGG, where the distance between every two points is the same. This main difference between the DGG (active) and the targeted regular degree grid is rectified by using a hamming window with search radius dependent on the latitude for the spatial resampling of the active microwave data.

Table 1: Major characteristics of passive and active microwave instruments and model product

	Passive microwave products							Active microwave products				Model product	
	SMMR	SSM/I	TMI	AMSR-E	AMSR2	Windsat	SMOS	AMI-WS	AMS-WS	ASCAT-A	ASCAT-B	GLDAS-2-Noah	GLDAS-2-Noah
Platform	Nimbus 7	DMSP	TRMM	Aqua	GCOM-W1	Coriolis	SMOS	ERS1/2	ERS2	MetOp-A	MetOp-B	---	---
Time period used	Jan 1979 – Aug 1987	Sep 1987 – Dec 2007	Jan 1998 – Dec 2013	Jul 2002 – Oct 2011	May 2012 – Dec 2017	Oct 2007 – Jul 2012	Jan 2010 – Dec 2017	Jul 1991 – Dec 2006	May 1997 – Feb 2007	Jan 2007 – Dec 2017	Nov 2012 – Dec 2017	Jan 1948 – Dec 2010	Jan 2000 – Jun 2018
Algorithm Product version	LPRM v05	LPRM v05	LPRM v05	LPRM v06	LPRM v06	LPRM v05	LPRM v06	WARP 5.4 P1R1	WARP 5.5 P1R1	WARP 5.8 P2R2	WARP 5.8 P2R2	V2.0	V2.1
Channel used for soil moisture	6.6 GHz	19.3 GHz	10.7 GHz	6.9/10.7 GHz	6.925/10.65 GHz	6.8/10.7 GHz	1.4 GHz	5.3 GHz	5.3 GHz	5.3 GHz	5.3 GHz	---	---
Original spatial resolution * (km²)	150×150	69 × 43	59 × 36	76 × 44	35 x 62	25 x 35	40 km	50 × 50	25 x 25	25 × 25	25 × 25	25 × 25	25 × 25
Spatial coverage	Global	Global	N40° to S40°	Global	Global	Global	Global	Global	Global	Global	Global	Global	Global
Swath width (km)	780	1400	780/897 after boost in Aug 2001	1445	1450	1025	600	500	500	1100 (550×2)	1100 (550×2)	---	---
Equatorial crossing time	Descending: 0:00	Descending: 06:30	Varies (non polar-orbiting)	Descending: 01:30	Descending 01:31	Descending 6:03	Ascending 6:00	Descending: 10:30	Desending 10:30	Descending: 09:30	Descending: 09:30	---	---
Unit	m^3m^{-3}	m^3m^{-3}	m^3m^{-3}	m^3m^{-3}	m^3m^{-3}	m^3m^{-3}	m^3m^{-3}	Degree of saturation (%)	Degree of saturation (%)	Degree of saturation (%)	Degree of saturation (%)	$kg\ m^{-2}$	$kg\ m^{-2}$

**For passive and active microwave instruments, this stands for the footprint spatial resolution.*

6.1.2 Temporal Resampling

The temporal sampling of the merged product is 1 day. The reference time for the merged dataset is set at 0:00 UTC. For each day starting from the time frame center at 0:00 UTC observations within ±12 hours are considered. The elaborated temporal resampling strategy firstly searches for the valid observation that is closest to the reference time. In case there are only invalid observations, which are flagged other than "0" (zero), within a certain time frame, the closest measurement among these invalid observations is selected. In the event that there are no measurements available at all within a time frame, no action is taken. This strategy results in data gaps when no observations within ±12 hours from the reference time are available. For the modelled soil moisture datasets, no resampling is required as they already include the reference time stamp of 0:00 UTC. The LPRM (passive) soil moisture estimates based on night-time (often the descending mode) observations are more reliable than those obtained during the day (often the ascending mode). This is mainly caused by the complexity to derive accurate estimates of the effective surface temperature during the day. For this reason, only night-time soil moisture observations from radiometers are used for the merged product.

During the temporal resampling stage, flagging is applied to the datasets where relevant information is available. For the LPRM products, the data is flagged for high VOD using the VOD fields provided in the data product. At v04.4 of the ESA CCI SM, where LPRM v6 is used for AMSR2 and SMOS, the thresholds above which VOD is considered 'high' are set based on the saturation point in the VOD signal for that sensor and band. This is the point at which the VOD value is considered to equal 100% vegetation signal.

6.2 Rescaling

Due to different observation frequencies, observation principles, and retrieval techniques, the contributing soil moisture datasets are available in different observation spaces. Therefore, before merging can take place at either level, the datasets need to be rescaled into a common climatology. The rescaling procedure is applied to the daily soil moisture values at three levels in the processing chain:

1) Rescaling of all the passive microwave soil moisture observations to the climatology of AMSR-E.
2) Rescaling of all the active microwave soil moisture observations to the climatology of ASCAT.
3) (Separately) Rescaling of all the active and passive microwave datasets to the climatology of GLDAS-Noah v2.1 which is available from the year 2000 onwards. Where there is an overlap between the sensors and v2.1 only the data in the overlap is used; where there is no overlap, the entire v2.1 time series is used.

Scaling is performed using cumulative distribution function (CDF) matching which is a well-established method for calibrating datasets with deviating climatologies (Drusch et al. 2005; Liu et al. 2007; Liu et al. 2011; Reichle et al. 2004). CDF-matching is applied for each grid point individually and based on piece-wise linear matching. This variation of the CDF-matching technique proved to be robust also for shorter time periods (Liu et al. 2011). The matching is shown by means of an example for a grid point centred at 41.375°N, 5.375°W. Figure 3 shows for this location the time series of soil moisture estimates from GLDAS-Noah, AMSR-E and ASCAT, respectively. CDF-matching for these time series is performed in the following way:

1. Time steps (0:00 UTC ±12h) are identified for which all data sets provide valid soil moisture values.
2. For the time-collocated data points CDFs are computed (Figure 3 a-c).
3. For each CDF curve the 0, 5, 10, 20, 30, 40, 50, 60, 70, 80, 90, 95 and 100 percentiles are identified.
4. Use the 13 percentiles of the CDF curves to define 12 segments. The CDF curves of these circled values are shown in Figure 4 a, b and c.
5. The 13 percentile values from the AMSR-E and ASCAT CDF curves are plotted against those of Noah (Figure 4 d and e) and scaling linear equations (e.g., slope and intercept) between two consecutive percentiles are computed.

$$slope_i = \frac{pref_{i+1} - pref_i}{psrc_{i+1} - psrc_i}$$

$$intercept_i = pref_i - (psrc_i * slope_i)$$

where i=1..12, is the number of the segments, and $pref$ is the percentile of the GLDAS-Noah data (reference), and $psrc$ is the percentile of either AMSR-E or ASCAT data (source) respectively.

6. The obtained linear equations are used to scale all observations of the target data set (i.e., also the time steps that do not have a corresponding observation in the reference data set) to the climatology of the reference data set (Figure 4 f).

$$sm_r = slope_i * sm + intercept_i$$

where sm_r is the rescaled soil moisture and sm is the original soil moisture value. $slope_i$ and $intercept_i$ are chosen depending on the sm value and its corresponding i-percentile.

The AMSR-E and ASCAT values outside of the range of CDF curves can also be properly rescaled, using the linear equation of the closest value.

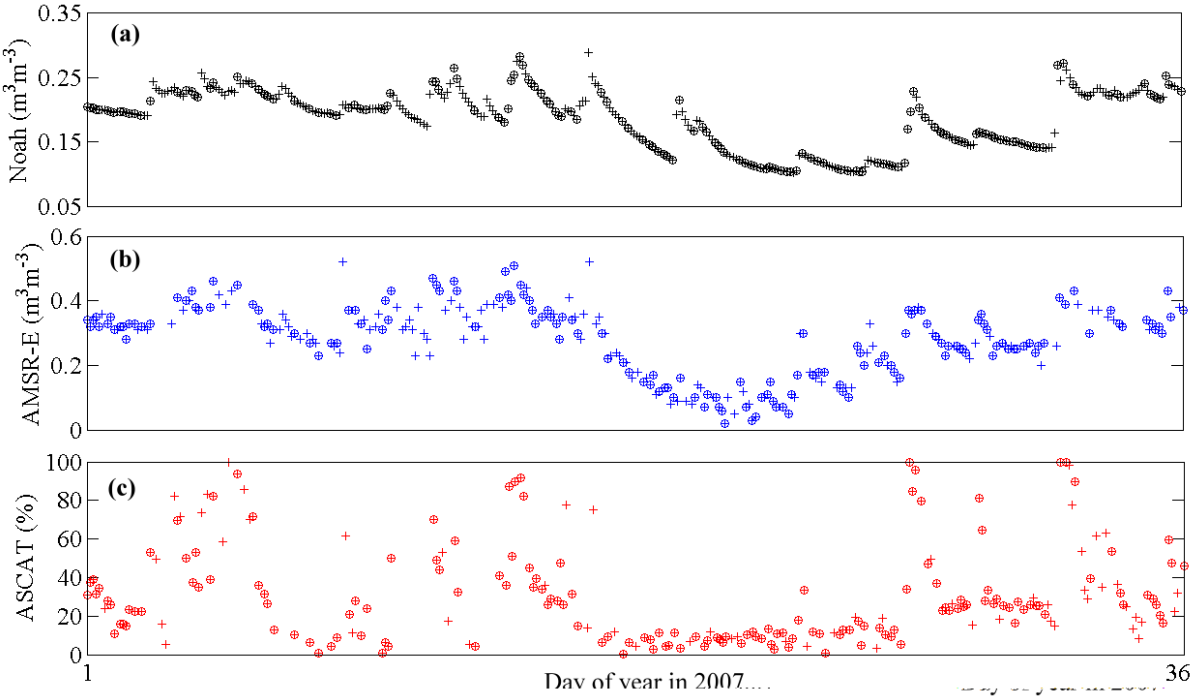

Figure 3: Time series of soil moisture estimates from (a) Noah, (b) AMSR-E and (c) ASCAT for a grid cell (centered at 41.375° N, 5.375° W) in 2007. Circles represent days when Noah, AMSR-E and ASCAT all have valid estimates. (Figure taken from Liu et al. 2011)

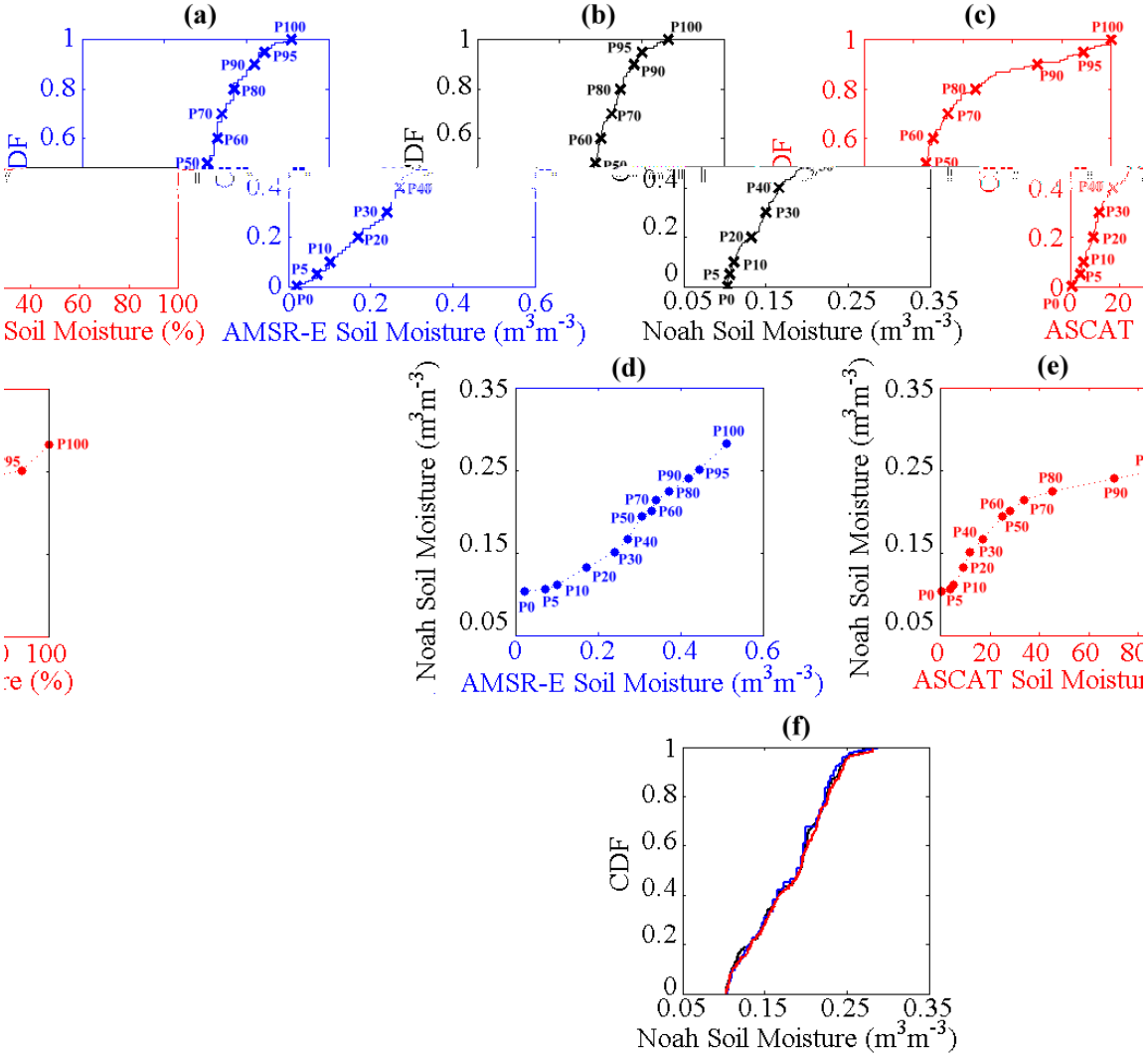

Figure 4: Example illustrating how the cumulative distribution function (CDF) matching approach was implemented to rescale original AMSR-E and ASCAT against Noah soil moisture product in this study. (a, b, c) CDF curves of AMSR-E, Noah and ASCAT soil moisture estimates for the grid cell shown in Fig. 2. (d) Linear regression lines of AMSR-E against Noah for 12 segments. (e) Same as (d), but for ASCAT and Noah. (f) CDF curves of Noah (black), rescaled AMSR-E (blue) and rescaled ASCAT (red) soil moisture products. (Figure taken from Liu et al. 2011)

6.3 Error characterization

Errors in the individual active and passive products are characterized by means of triple collocation analysis. These errors are used both for estimating the merging parameters and for characterizing the errors of the merged product (see section 6.4).

6.3.1 Triple collocation analysis

Triple collocation analysis is a statistical tool that allows estimating the individual random error variances of three data sets without assuming any of them acting as supposedly accurate reference (Gruber et al. 2016). This method requires the errors of the three data sets to be uncorrelated, therefore triplets always comprise of (i) an active data set, (ii) a passive data set, and (iii) the GLDAS-Noah land surface model, which are commonly assumed to fulfil this requirement (Dorigo et al. 2010). Error variance estimates are obtained as:

$$\sigma_{\varepsilon_a}^2 = \sigma_a^2 - \frac{\sigma_{ap}\sigma_{am}}{\sigma_{pm}}$$
$$\sigma_{\varepsilon_p}^2 = \sigma_p^2 - \frac{\sigma_{pa}\sigma_{pm}}{\sigma_{am}} \qquad \textit{Eqn. 6-1}$$

where σ_ε^2 denotes the error variance; $\sigma^2$and σ denote the variances and covariances of the data sets; and the superscripts denote the active (a), the passive (p), and the modelled (m) data sets, respectively. For a detailed derivation see (Gruber et al. 2016). Notice that these error estimates represent the average random error variance of the entire considered time period, which is commonly assumed to be stationary. Furthermore, the soil moisture uncertainties of the three products (ACTIVE, PASSIVE, and COMBINED) are determined by the above equations.

6.4 Error gap-filling

TCA does not provide reliable error estimates in all regions, mainly if there is no significant correlation between all members of the triplet, which often happens for example in high-latitude areas or in desert areas. TCA error estimates are therefore disregarded in case of insignificant Pearson correlation (p-value < 0.05) between any of the data sets. In these areas, error estimates are derived from the mean VOD (derived from AMSR-E in the entire mission period) at that particular location:

$$SNR_x = \sum_{\{i=0\}}^{N} a_i VOD_x^i \qquad \textit{Eqn. 6-2}$$

Where the subscript denotes the spatial location; and the parameters a_i are derived from a global polynomial regression between VOD and TCA based error estimates at locations where they are considered reliable (i.e., all data sets are significantly correlated). For TMI and

WINDSAT third order polynoms (N=3) are used and for all other sensors second order polynoms (N=2) are used, which was empirically found to provide the best regression results.

6.5 Merging

The merging procedure consists of (1) merging the original passive microwave product into the PASSIVE product, (2) merging the original active microwave products into the ACTIVE product, and (3) merging the original active and passive microwave products into the COMBINED product. The merging is performed by means of a weighted average which takes into account the error properties of the individual data sets that are being merged. Such weighted average is calculated as

$$\Theta_m = \sum_{i=1}^{N} w_i \cdot \Theta_i \qquad \textit{Eqn. 6-2}$$

where Θ_m denotes the merged soil moisture product; Θ_i are the soil moisture products that are being merged, and w_i are the merging weights.

6.5.1 Weight estimation

Per definition, the optimal weights for a weighted average are determined by the error variances of the input data sets and write as follows:

$$w_i = \frac{\sigma_{\varepsilon_i}^{-2}}{\sum_{j=1}^{N} \sigma_{\varepsilon_j}^{-2}} \qquad \textit{Eqn. 6-3}$$

where the superscripts denote the respective data sets; i is the data set for which the weight is being calculated; and N is the total number of data sets which are being averaged. The required error variances are calculated using Eqn. 6-3. Notice that error covariance terms are neglected as they cannot be estimated reliably.

It should be mentioned that the above definition of the weights based on error variances assumes all data sets to be in the same data space. However, data sets usually vary in their signal variability due to algorithmic differences, varying signal frequencies, etc. Therefore, conceptually, it is more appropriate to define relative weights in terms of the data sets SNR properties rather than of their error variance (Gruber et al. 2017). Nevertheless, the actual merging requires a harmonization of the data sets into a common data space, which in the case of the CCI SM data set is done using the CDF matching approach described in Section 6.2. Therefore, the calculation of the weights using Eqn. 6-3 suffices, keeping in mind that they represent rescaled error variances of rescaled data sets.

6.5.2 *Merging passive microwave products*

Differences in sensor specifications, particularly in microwave frequency and spatial resolution, result in different absolute soil moisture values from SMMR, SSM/I, TMI and AMSR-E. Even though SMMR and AMSR-E have a similar frequency (i.e., C-band), their absolute values are different. Therefore, a Spearman and Pearson correlation analysis was performed between the different soil moisture products to identify differences and correspondences between the data sets (Liu et al. 2012). Based on this analysis, the AMSR-E soil moisture retrievals were identified as more accurate than the other passive products due to the relatively low microwave frequency and high temporal and spatial resolution of the sensor. Thus, soil moisture retrievals from AMSR-E are selected as the reference to which soil moisture retrievals from SMMR, SSM/I, TMI, WindSat, and SMOS are rescaled and merged on a pixel basis according to the following steps. AMSR2 data were not rescaled as there is no overlapping time period between AMSR-E and AMSR2.

Merging SSM/I and TMI with AMSR-E

1. Rescale original TMI against the AMSR-E reference using the piece-wise linear cumulative distribution function (CDF) matching technique (Section 6.2) based on their overlapping period (Figure 5a),
2. Decompose SSM/I and AMSR-E time series into their own seasonality and anomalies (Figure 5b). This is done for their overlapping period from July 2002 through December 2007. The seasonality for each sensor was calculated by taking the average of the same day of the year for their overlapping period. The seasonality ($\overline{SM}$) is one time series of 366 values, one value for each day of the year (*DOY*):

$$\overline{SM}_{DOY} = \left(\sum_{YR=2002}^{2007} SM_{DOY}^{YR} \right) \Big/ N \qquad \text{Eqn. 6-4}$$

where *YR* represents the year 2002 through 2007; *N* represents the number of valid soil moisture retrievals. The value of $\overline{SM}_{366}$ is only taken from the year 2004 as that is the only leap year (i.e., 366 days) between 2002 and 2007. The anomalies (*ANO*) over their individual entire periods were obtained by removing the sensor's seasonality $\overline{SM}$ from the original (*ORI*) time series:

$$ANO_{DOY}^{YR} = ORI_{DOY}^{YR} - \overline{SM}_{DOY} \qquad \text{Eqn. 6-5}$$

where *YR* represents the year 1987 through 2007 for SSM/I and 2002 through October 2011 for AMSR-E.

3. Rescale “anomalies of SSM/I” against “anomalies of AMSR-E” using the piece-wise linear CDF matching technique (Figure 5c).
4. Add the AMSR-E seasonality to the “rescaled SSM/I anomalies” (from Step 3) and obtain reconstructed SSM/I (Figure 5d).
5. Merge the reconstructed SSM/I, rescaled TMI, and original AMSR-E to obtain the merged SSM/I-TMI-AMSR-E dataset (Figure 5e). The lower the measurement frequency, the more accurate soil moisture retrievals can be expected. Therefore AMSR-E is used for July 2002 – December 2008 and the rescaled TMI is used for January 1998 – June 2002 between N40^{o} and S40^{o}. Otherwise the reconstructed SSM/I is used.

Merging SMMR with SSM/I-TMI-AMSR-E

The overlapping period between SMMR and other sensors is too short to perform the rescaling as conducted on retrievals from other sensors. In order to incorporate SMMR (1979 – 1987) soil moisture retrievals into the merged product, we assumed that the dynamic range of SMMR retrievals is the same as the range of merged SSM/I-TMI-AMSR-E dataset. Following this assumption, we produced the rescaled SMMR (Nov 1978 to July 1987) by matching the CDF curve of SMMR against that of the merged SSM/I–TMI–AMSR-E dataset for each grid point. The CDF curve is calculated based on all observation of both data sets. Together with the merged SSM/I-TMI-AMSR-E dataset, we obtained the merged SMMR-SSM/I-TMI-AMSR-E soil moisture product covering the period Nov 1978 – Sep 2007 (Figure 5). It should be emphasized that the CDF matching process changes the absolute values of SMMR, SSM/I and TMI products, but does not change the relative dynamics of the original retrievals, which is demonstrated in Liu et al. (2011).

Table 2 Used passive sensors in the PASSIVE product

Time Period	Passive Sensors (mode: ascending (a) or descending (d))
01/11/1978 – 31/07/1987	SMMR (d)
01/09/1987 – 31/12/1997	SSM/I (a)
01/01/1998 – 18/06/2002	SSM/I (a) [90N – 40N], [90S – 40S], TMI (d) [40N – 40S]
19/07/2002 – 30/09/2007	AMSR-E (d)
01/10/2007 – 14/01/2010	AMSR-E (d), Windsat (d)
15/01/2010 – 04/10/2011	AMSR-E (d), WindSat (d), SMOS (a)
05/10/2011 – 30/06/2012	WindSat (d), SMOS (a)
01/07/2012 – 30/06/2018	SMOS (a), AMSR2 (d)

Merging SMOS, WindSat, and AMSR2 with SMMR-SSM/I-TMI-AMSR-E

WindSat data (1 October 2007 to 31 June 2012) bridge the operational time gap between AMSR-E, which failed to deliver data from 4 October 2011 onwards, and AMSR2, for which data are available from 02 July 2012 onward. SMOS data in ascending satellite mode are available from 1 July 2010 to 8 May 2015. The CDFs between WindSat and AMSR-E, and SMOS and AMSR-E are calculated based on their respective overlapping time periods with AMSR-E. Within the time period from 1 October 2007 to May 2015 there are various combinations of data overlap. Figure 2, Table 2, and Figure 8b illustrate these overlaps. The data periods AMSR-E & WindSat (1 October 2007 to 30 June 2010), AMSR-E & WindSat & SMOS (1 July 2010 to 3 October 2011), WindSat & SMOS (4 October 2011 to 30 June 2012), are then extended with AMSR2 & SMOS (1 July 2012 to 30 June 2018). The resulting product hereafter is referred to as the PASSIVE product. The following paragraph describes the in more detail the process of merging these datasets, when more than one sensor is used.

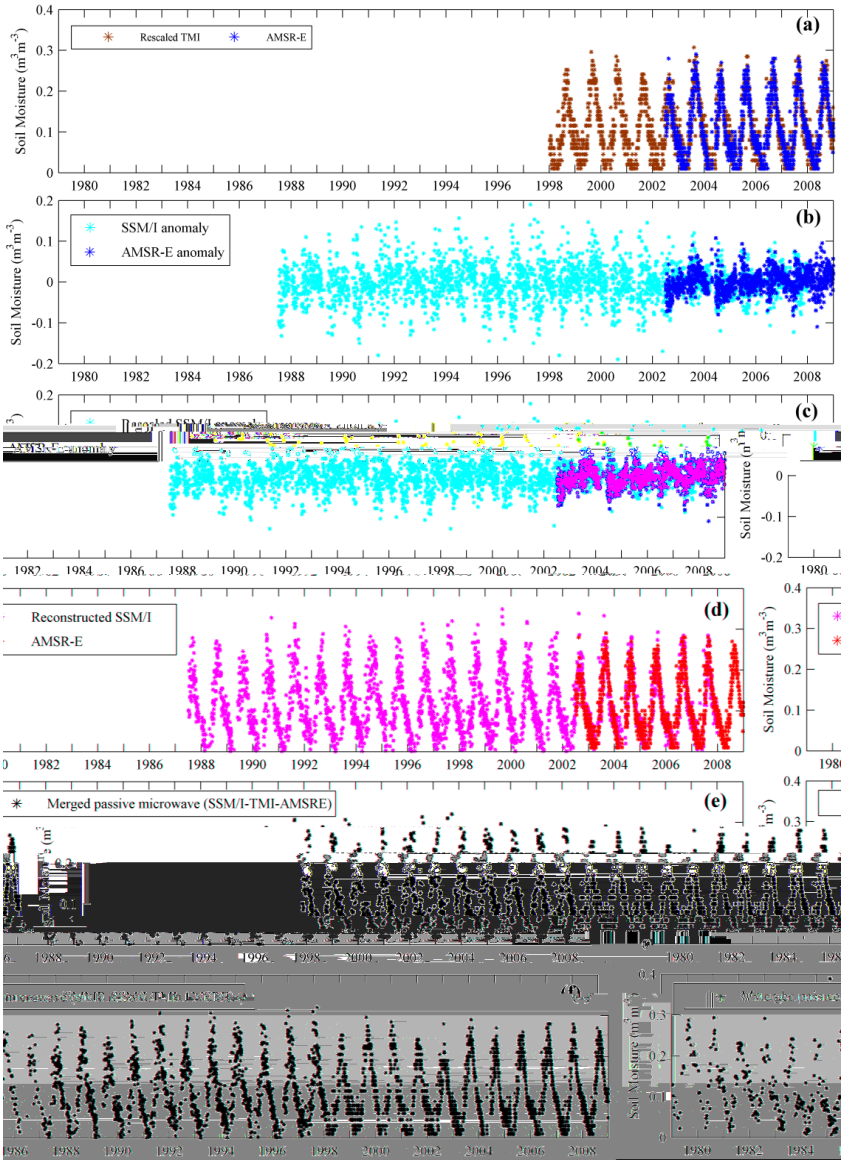

Figure 5: Example illustrating how (a) the TMI was rescaled against AMSR-E, (b-e) the SSM/I anomalies were rescaled against AMSRE-E anomalies, reconstructed and merged with rescaled TMI and AMSR-E, and (e) the SMMR was rescaled and merged with the others. The grid cell is centred at 13.875°N, 5.875°W.). (Image courtesy Liu et al. 2012)

Merging in periods where more than one sensor is used

As it can be seen from Figure 8 there are periods where more than one passive dataset is available, i.e., AMSR-E & WindSat. In these periods, a weighted average of the respective sensors is used to construct the merged PASSIVE product (see Eqn. 6-5). Error estimates are obtained from triple collocation analysis (see section 6.3) using ASCAT/ERS and GLDAS-Noah data to complement the respective triplets.

Notice that soil moisture estimates of the various sensors are not available every day, hence there are certain dates during the overlapping periods on which not all data sets provide a valid estimate to calculate the weighted average. In such cases, the weights are re-distributed amongst the remaining data sets, again based on their relative SNR properties.

However, this re-distribution of weights could significantly worsen data quality on these days because of the increasing contribution of measurements which initially would have had a low weight due to their (relatively) low SNR. Therefore, soil moisture estimates in the merged product on days where not all data sets provide valid estimates are set to NaN, if the sum of the initial weight of the remaining data sets is lower than 1/(2N) where N is the total number of data sets that are potentially available for the corresponding merging period. This threshold has been derived empirically to provide a good trade-off between temporal measurement density and average data quality.

6.5.3 Merging active microwave products

Different sensor specifications between ERS1/2 and ERS2 (e.g. spatial resolution) need to be compensated by using the same rescaling techniques performed on the radiometer data sets. The CDF curves for ERS2 are calculated based on the overlap with ERS1/2. Rescaling ERS2 against ERS1/2 and then merging them generates the AMI-WS active data set, which is subsequently scaled and merged to the MetOp-A ASCAT data (Figure 2).

Table 3 and Figure 8a show the sensors used in the ACTIVE product for the individual time periods.

Table 3 Used active sensors in the ACTIVE product

Time Periods	Active Sensors
05/08/1991 – 19/05/1997	ERS1/2 (AMI-WS)
20/05/1997 – 17/02/2003	ERS2 (AMI-WS)
18/02/2003 – 31/12/2006	ERS1/2 (AMI-WS)
01/01/2007 – 05/11/2012	MetOp-A ASCAT
06/11/2012 – 31/12/2017	MetOp-A ASCAT, MetOp-B ASCAT

An example of a soil moisture time series from AMI-WS ERS1/2 and MetOp-A ASCAT for the grid point centred at 13.875°N, 5.875°W (Niger River basin in southern Mali) is shown in Figure 6, where the AMI-WS ERS1/2 is labelled as SCAT to denote its predecessor role to ASCAT. The AMI-WS ERS1/2 and MetOp-A ASCAT soil moisture variations are scaled between the lowest

(0%) and highest (100%) values over their individual operational period. The limited overlap in time (i.e., a few months) and space (i.e. only Europe, Northern America and Northern Africa) rules out the global adjustment method based on the information of their overlapping period, such as applied between TMI and AMSR-E. Figure 6 also shows the evident AMI-WS ERS1/2 data gap from 2001 to 2003.

As retrievals from MetOp-A ASCAT and AMI-WS capture similar seasonal cycles (Liu et al. 2011), we assume that their dynamic ranges are identical and use for each grid point the CDF curves of both datasets to rescale AMI-WS to MetOp-A ASCAT before merging them (Figure 6b). MetOp-A ASCAT data from 1 January 2007 to 5 November 2012 are joined with AMI-WS data from 5 August 1991 to 31 December 2006. In the time period from 6 November 2012 to 30 June 2018 MetOp-A ASCAT and MetOp-B ASCAT data are available. These two datasets are merged by applying the arithmetic average for locations, where both observations are available, otherwise either one of the two is then used. Joining AMI-WS& MetOp-A ASCAT from 5 August 1991 to 5 November 2012 with MetOp-A ASCAT & MetOp-B ASCAT from 6 November 2012 to 30 June 2018 generates the ACTIVE product (Figure 2 and Figure 8a).

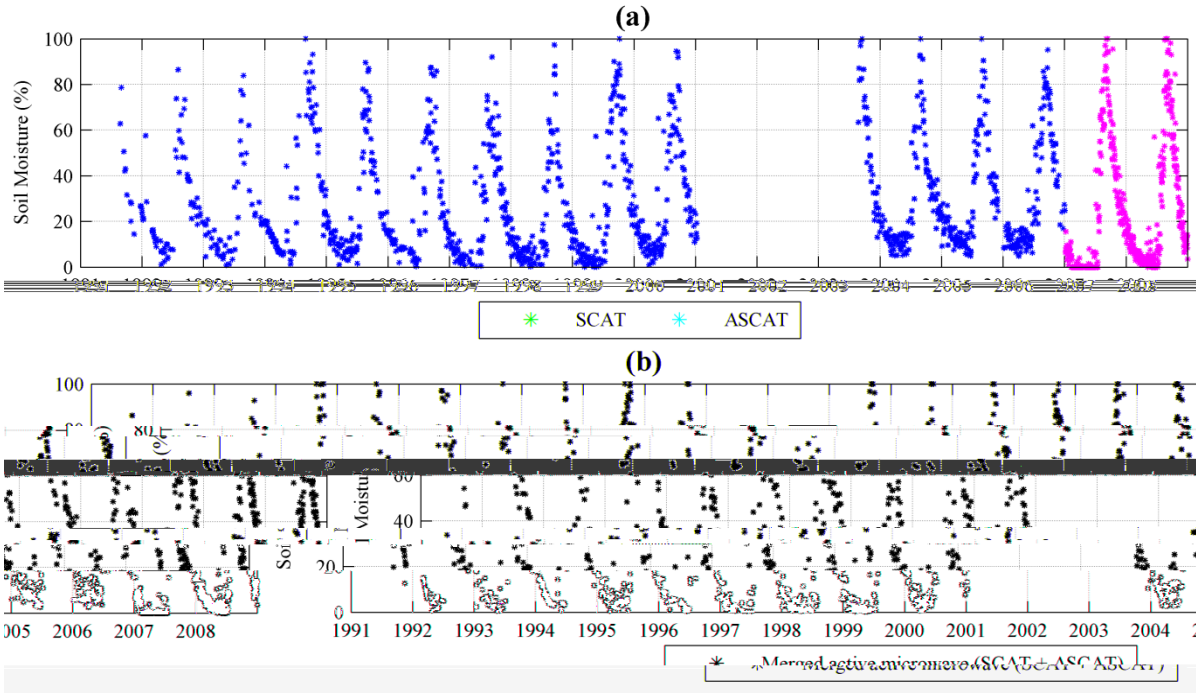

Figure 6: Example illustrating fusion of ERS1/2 (SCAT) with ASCAT. Note the data gap from 2001 – 2003, which will be filled by ERS2 data. The grid point is centred at 13.875°N, 5.875°W.). (Image courtesy Liu et al. 2012)

6.5.4 *Merging passive and active microwave products*

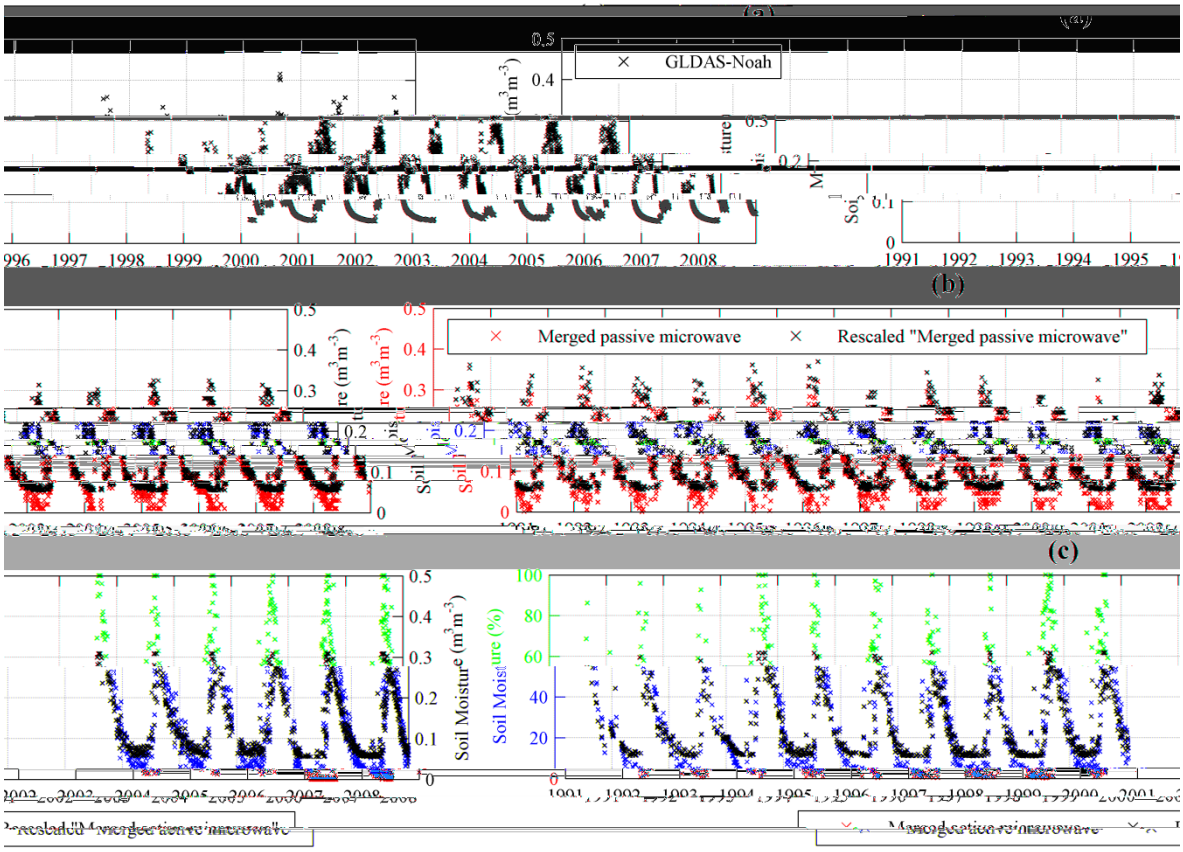

Figure 7: Rescaling the merged passive and active microwave product against the GLDAS-1-Noah simulation. (a) GLDAS-1-Noah soil moisture; (b) merged passive microwave product and one rescaled against GLDAS-1-Noah; (c) same as (b) but for active microwave product. The grid cell is centred at 13,875°N, 5.875°W.). (Image courtesy Liu et al. 2012)

For generating the combined product, climatologies of all passive and active level 2 data sets are first harmonized by rescaling against GLDAS-1 (see Sec. 6.2). Considering the covering period of each microwave instrument we divided the entire time period (1978 – 2018) into eleven segments. Table 4 list these time periods, and Figure 8c illustrates also the spatial sensor usage at global scale.

Table 4 Used sensors in individual time periods. Note that MetOp-B ASCAT data are available from 06. November 2012 onwards.

Time Periods	Active Sensors	Passive Sensors
01/11/1978 – 31/08/1987	N/A	SMMR
01/09/1987 – 04/08/1991	N/A	SSM/I
05/08/1991 – 31/12/1997	AMI-WS	SSM/I
01/01/1998 – 18/06/2002	AMI-WS	SSM/I [90N-40N], [90S-40S], TMI [40N-40S]
19/06/2002 – 31/12/2006	AMI-WS	AMSR-E
01/01/2007 – 30/09/2007	MetOp-A ASCAT	AMSR-E
01/10/2007 – 30/06/2010	MetOp-A ASCAT	AMSR-E, WindSat
15/07/2010 – 04/10/2011	MetOp-A ASCAT	AMSR-E, WindSat, SMOS
05/10/2011 – 30/06/2012	MetOp-A ASCAT	WindSat, SMOS
01/07/2012 – 30/06/2018	MetOp-A ASCAT, MetOp-B ASCAT	AMSR2, SMOS

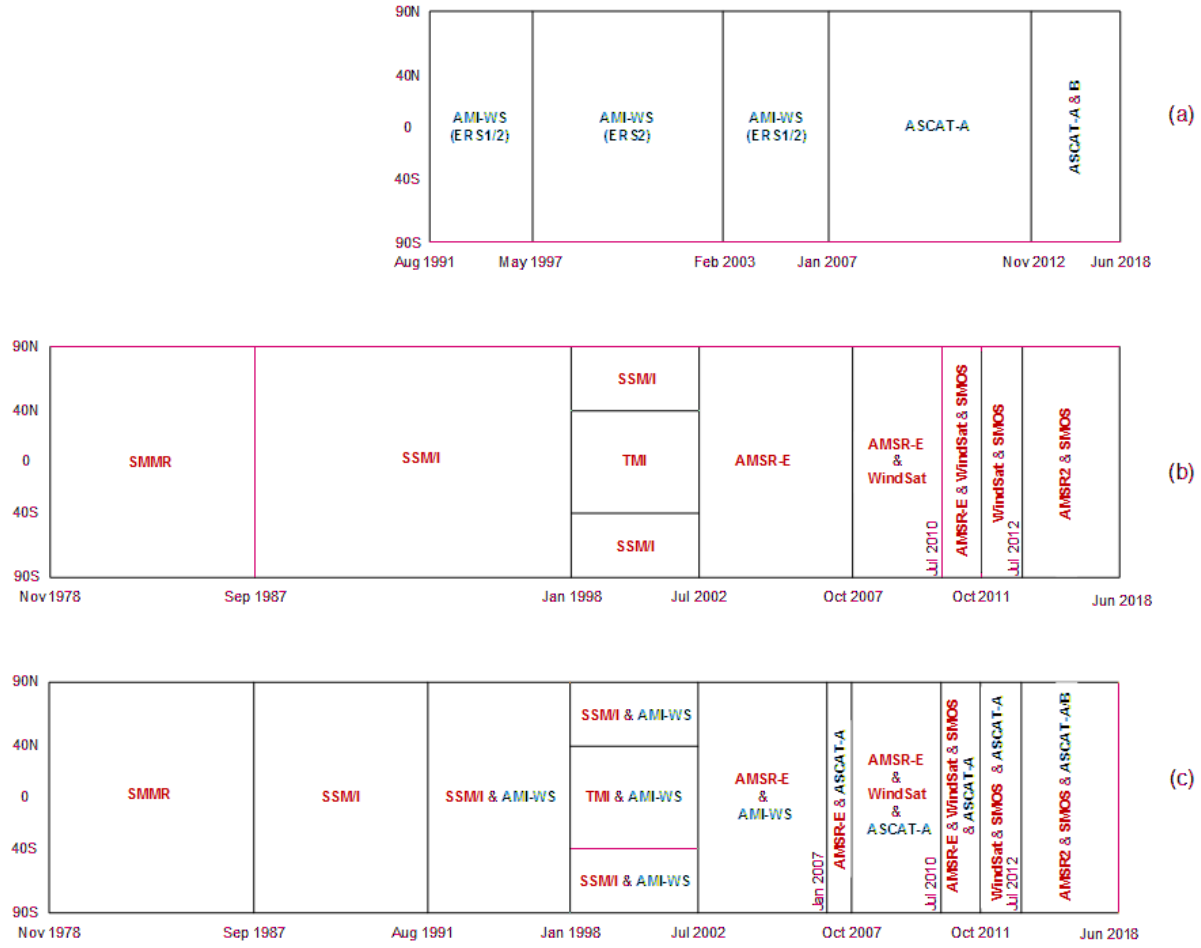

Figure 8 Spatial and temporal coverage of soil moisture products from different sensors in the CCI SM v04.4 COMBINED product. Figure adapted from (Dorigo et al. 2017).

Similar to the generation of the PASSIVE product, relative weights at each time step are derived from the TCA- or VOD-regression based error estimates for each individual sensor. Depending on how many sensors are available within a particular period, a (1/2N) threshold for the minimum weight of a particular sensor was applied if not all sensors provide a soil moisture estimate at that day.

7 Known Limitations

7.1 Passive merged CCI product

7.1.1 Using night-time observations only

For the current version of the merged passive product only descending overpasses, corresponding to night-time / early morning observations, were considered. This is because near surface land surface temperature gradients are regarded to be reduced at night leading to more robust retrievals (Owe et al. 2008). However, recent studies (Brocca et al. 2011) suggest that for specific land cover types day-time observations may provide more robust retrievals than night-time observations, although the exact causes are still unknown. If day-time observations could be introduced to the blended product, this would significantly increase the observation density.

7.2 Intercalibration of AMSR-E and AMSR2

As AMSR-E fails to deliver data since 04 October 2011 the continuity of the passive radiometer data is prolonged by using the WindSat and AMSR2 data sets. The Passive product is extended by using WindSat to bridge the time gap between AMSR-E and AMSR2. A intercalibration technique was developed to adjust WindSat soil moisture to AMSR-E and AMSR2 to the adjusted Windsat data (Parinussa et al. 2015). However, the overlapping period use to compute the calibration constants was very short and need to be updated using a larger time window. Alternatively, JAXA announced to make an improved intercalibrated AMSR2 product available, which, if outperforming the empirical intercalibration used so far, will be used to generate level 2 AMSR2 LPRM soil moisture estimates.

7.3 Active Product

7.3.1 Intercalibration of ERS and ASCAT

The generation of the ERS and ASCAT products is still based on their individual time series. The merged ERS + ASCAT could significantly profit from an appropriate Level 1 intercalibration. Besides improving the quality of the individual measurements this would improve the robustness of the calculation of the dry and wet references.

7.3.2 Data gaps

Similar as for the passive products, merging ERS and ASCAT into a merged dataset is based on a strict separation in time. Gaps in ASCAT time series can be potentially filled with ERS observations, although the spatial and temporal overlap between both sensors is limited.

8 Scientific Advances under Investigation

8.1 All products

8.1.1 Separate blending of climatologies and anomalies

Currently the SNR-based merging scheme applies a relative weighting of data sets based on their relative error characteristics. However, studies have shown that different spectral components may be subject to different error magnitudes (Su et al. 2015, Draper et al. 2016). Therefore, we will investigate the feasibility of blending the climatologies and the anomalies of the data sets separately.

8.1.2 Improved sensor inter-calibration

Currently, inter-calibration between active and passive data sets is done using CDF-matching against a long-term consistent land surface model. However, in order to achieve a full model-independence of the CCI SM products, we will investigate alternative inter-calibration approaches, for instance using lagged-variable based approaches or homogeneity tests (Su et al. 2015, 2016)

8.1.3 Data density and availability

In the current versions, gaps are only filled if the weight of the available product is above a relatively crudely defined empirical threshold. This threshold will be refined to find a best compromise between data density and product accuracy.

8.2 PASSIVE product

8.2.1 Using night-time observations only

Based on extensive product validation and triple collocation we will try to address the uncertainty of both modes. Based on these results we will decide how both observations modes can be considered in the generation of a single merged passive product, potentially leading to improved observation frequency with respect to the single descending mode used in the CCI SM product. An important step in this step was made by Parinussa et al. (2016).

8.3 ACTIVE product

8.3.1 Intercalibration of ERS and ASCAT

It is currently investigated how ERS and ASCAT backscatter values can be reliably intercalibrated directly so that the WARP TU Wien retrieval algorithm can be directly applied to the entire intercalibrated time series.

8.3.2 Data gaps

In the framework of the project it will be studied if gaps in the ASCAT time series, as shown in 7.3.2, can be potentially filled with ERS.

8.4 COMBINED product

There are currently no scientific advances under investigation. For details of recently undertaken work including quality assessment of the combined product, please refer to (Dorigo et al. 2017)

9 References

Brocca, L., Hasenauer, S., Lacava, T., Melone, F., Moramarco, T., Wagner, W., Dorigo, W., Matgen, P., Martínez-Fernández, J., Llorens, P., Latron, J., Martin, C., & Bittelli, M. (2011). Soil moisture estimation through ASCAT and AMSR-E sensors: An intercomparison and validation study accross Europe. *Remote Sensing of Environment*, 3390-3408

Dorigo, W., Wagner, W., Albergel, C., Albrecht, F., Balsamo, G., Brocca, L., Chung, D., Ertl, M., Forkel, M., Gruber, A., Haas, E., Hamer, P.D., Hirschi, M., Ikonen, J., de Jeu, R., Kidd, R., Lahoz, W., Liu, Y.Y., Miralles, D., Mistelbauer, T., Nicolai-Shaw, N., Parinussa, R., Pratola, C., Reimer, C., van der Schalie, R., Seneviratne, S.I., Smolander, T., & Lecomte, P. (2017). ESA CCI Soil Moisture for improved Earth system understanding: State-of-the art and future directions. *Remote Sensing of Environment*

Dorigo, W.A., Scipal, K., Parinussa, R.M., Liu, Y.Y., Wagner, W., de Jeu, R.A.M., & Naeimi, V. (2010). Error characterisation of global active and passive microwave soil moisture datasets. *Hydrology and Earth System Sciences, 14*, 2605-2616

Drusch, M., Wood, E., & Gao, H. (2005). Observation operators for the direct assimilation of TRMM microwave imager retrieved soil moisture. *Geophysical Research Letters, 32*, L15403

Gruber, A., Dorigo, W., Crow, W., & Wagner, W. (2017). Triple Collocation-Based Merging of Satellite Soil Moisture Retrievals. *IEEE Transactions of Geoscience and Remote Sensing*

Gruber, A., Su, C.H., Zwieback, S., Crowd, W., Dorigo, W., & Wagner, W. (2016). Recent advances in (soil moisture) triple collocation analysis. *International Journal of Applied Earth Observation and Geoinformation, 45*, 200-211

Liu, Y., de Jeu, R.A.M., van Dijk, A.I.J.M., & Owe, M. (2007). TRMM-TMI satellite observed soil moisture and vegetation density (1998-2005) show strong connection with El Nino in eastern Australia. *Geophysical Research Letters, 34*, Art. No. L15401

Liu, Y.Y., Dorigo, W.A., Parinussa, R.M., De Jeu, R.A.M., Wagner, W., McCabe, M.F., Evans, J.P., & Van Dijk, A.I.J.M. (2012). Trend-preserving blending of passive and active microwave soil moisture retrievals. *Remote Sensing of Environment, 123*, 280-297

Liu, Y.Y., Parinussa, R.M., Dorigo, W.A., de Jeu, R.A.M., Wagner, W., van Dijk, A., McCabe, F.M., & Evans, J.P. (2011). Developing an improved soil moisture dataset by blending passive and active microwave satellite-based retrievals. *Hydrology and Earth System Sciences, 15*, 425-436

Owe, M., de jeu, R., & Holmes, T. (2008). Multisensor historical climatology of satellite-derived global land surface moisture. *Journal of Geophysical Research-Earth Surface, 113*, F01002

Parinussa, R.M., Holmes, T.R.H., Wanders, N., Dorigo, W., & de Jeu, R.A.M. (2015). A preliminary study towards consistent soil moisture from AMSR2. *Journal Of Hydrometeorology, 16*, 932–947

Reichle, R.H., Koster, R.D., Dong, J., & Berg, A.A. (2004). Global Soil Moisture from Satellite Observation, Land Surface Models, and Ground Data: Implications for Data Assimilation. *Journal Of Hydrometeorology, 5*, 430-442

Rodell, M., Houser, P.R., Jambor, U., Gottschalck, J., Mitchell, K., Meng, C.J., Arsenault, K., Cosgrove, B., Radakovich, J., Bosilovich, M., Entin, J.K., Walker, J.P., Lohmann, D., & Toll, D. (2004). The Global Land Data Assimilation System. *Bulletin of the American Meteorological Society, 85*, 381-394